

Proposed low energy model Hamiltonian for spin-gapped system CuTe_2O_5 : A NMTO-downfolding study

H. Das, T. Saha-Dasgupta

Department of Material Sciences, S. N. Bose National Center for Basic Sciences, JD-III, Salt Lake City, Kolkata 700 098, India

(Dated: May 26, 2019)

Using muffin tin orbital (MTO) based NMTO-downfolding technique we analyze the electronic structure of the low-dimensional quantum spin system CuTe_2O_5 which has been recently investigated (J. Deisenhofer *et al*, Phys. Rev. B, **74** (2006) 174421) in terms of susceptibility and electron spin resonance measurements. Our study indicate that contrary to the findings by Deisenhofer *et al*, the system may be described as a two dimensional coupled dimer system, with different dominant interactions than those identified by Deisenhofer *et al*.

PACS numbers:

I. INTRODUCTION

Significant amount of effort both experimentally and theoretically has been devoted in recent years in understanding the behavior of systems that belong to the class of low-dimensional quantum spin compounds. A crucial information that goes in to study of these compounds is the information of the underlying spin model. In this study we investigate the underlying spin model of the compound CuTe_2O_5 which has caught attention very recently, within the framework of the Nth order muffin-tin orbital (NMTO)-downfolding technique.

CuTe_2O_5 is structurally a Cu(II)-dimer system. The magnetic susceptibility of CuTe_2O_5 show a maximum at $T_{max}=56.5$ K and an exponential drop below a temperature of ≈ 10 K signaling the opening of a spin gap. The high temperature susceptibility data corresponds to a Curie-Weiss temperature of $\theta=41$ K¹. The electron spin resonance (ESR) data suggested that structural dimers of CuTe_2O_5 do not coincide with the magnetic dimers². Fitting of the susceptibility data using different models, such as a pure dimer model, the alternating spin-chain model and the modified Bleaney-Bowers model, show that in CuTe_2O_5 the inter-dimer exchange coupling is of the same order of magnitude as the intra-dimer coupling. A detailed investigation of the magnetic exchange paths by Deisenhofer *et al*, using extended Huckel tight binding (EHTB) electronic structure calculations show that the strongest interaction (J_6) to be of antiferromagnetic supersuperexchange (SSE) type mediated by O-Te-O bridges and second strongest (J_1) to be the antiferromagnetic SE interaction within the structural dimer Cu_2O_{10} , yielding a ratio $J_1/J_6=0.59^2$. Based on these findings the authors propose an alternating spin chain model as the simplest possible model for CuTe_2O_5 . In the following, we investigate this proposition in terms of first principles density functional theory (DFT).

II. CRYSTAL STRUCTURE

CuTe_2O_5 crystallize in the monoclinic structure with space group P21/c and lattice parameters $a=6.871$ Å, $b=9.322$ Å, $c=7.602$ Å, $\beta=109.08^\circ$ ³. The system is built out of CuO_6 distorted octahedra (Fig-1a), given by Cu^{2+} ion surrounded by six inequivalent oxygens O1, O2, O3, O4, O5, O5'. Each CuO_6 octahedron is elongated along the O2-O5' axis, with distances $\text{Cu-O5}'=2.303$ Å and $\text{Cu-O2}=2.779$ Å. The Cu-O distances from other four plane oxygen ions range from $\text{Cu-O5}=1.948$ Å to $\text{Cu-O3}=1.969$ Å. Two neighboring CuO_6 octahedra edge share to form Cu_2O_{10} , a structural dimer (see Fig-1b) and the oxygen octahedra of two Cu^{2+} ions within an structural dimer are rotated by 180° against each other.

The structural dimers form a chain like structure running approximately along crystallographic c axis while the chains are arranged along the approximate crystallographic b axis (see Fig-2). The Te1 atoms are situated between two successive Cu(II)-structural dimer chains, while the Te2 atoms are situated in between two Cu_2O_{10} structural dimers along a particular chain. The local oxygen environment of Te atoms form a TeO_4 tetrahedra (see Fig-1c). The layers containing these chains in approximate bc plane are stacked along the approximate crystallographic a axis with little connection between each other.

III. BAND STRUCTURE

Fig-3 and Fig-4 show the non-spin polarized band dispersion and density of states (DOS) respectively, of the system CuTe_2O_5 , obtained from electronic structure calculations in the linear muffin tin orbital basis⁴ within the framework

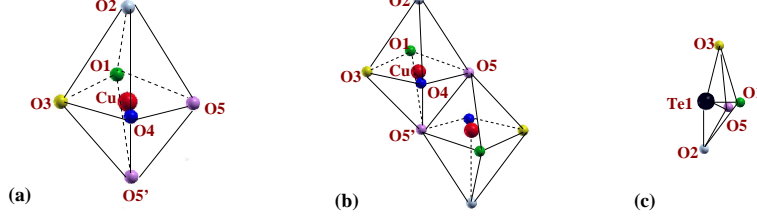


FIG. 1: Building units of CuTe₂O₅. (a)CuO₆-distorted octahedron. (b)Cu₂O₁₀-structural dimer unit. (c)TeO₄-tetrahedra

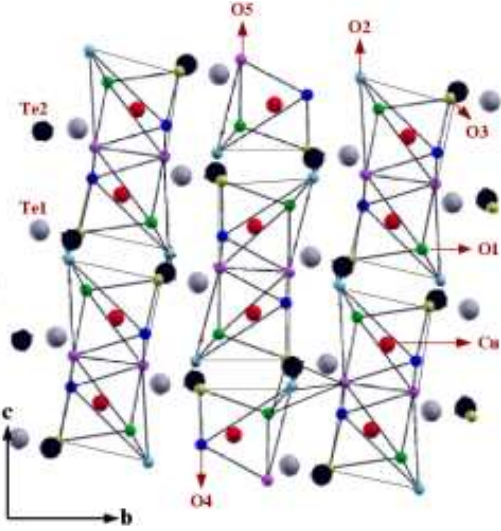


FIG. 2: Crystal structure of CuTe₂O₅ (space group P21/c) . The largest balls represent Te1 and Te2. Te1 and Te2 are shown in grey and black colors respectively. Cu atoms are of medium size and shown in red colors. The smallest balls denote the oxygen atoms, there are five inequivalent oxygen atoms in an unit cell, denoted by balls colored green(O1), cyan(O2), yellow(O3), blue(O4) and magenta(O5). The Cu₂O₁₀ dimer units are separated by TeO₄ units. Only one of the TeO₄ unit is shown for clarity.

of local density approximation (LDA). The orbital contributions to the valence and conduction bands in the band dispersions and the DOS were determined in terms of the orbital projected band structure (fatbands), calculated in the local coordinate system defined as local z-axis pointing along Cu-O₂ bond and local y-axis pointing approximately along the Cu-O₅ bond, and the partial density of states (PDOS), respectively.

The predominant features of the band structure is the isolated complex of four bands crossing the Fermi level (E_f), formed by Cu- $d_{x^2-y^2}$ orbitals, contributed by each Cu atom in the unit cell, admixed with O-p states. These bands are half filled and separated from the low lying O-p and other Cu character dominated valence bands by a gap of about 0.83 eV and from the Te-p dominated high lying conduction bands by another gap of about 2.18 eV, with the zero of energy set at the LDA Fermi level. We note that in the low energy scale, the LDA calculation leads to four half-filled bands crossing the Fermi level, *ie*, to a metallic state. Introduction of missing correlation effect beyond LDA is expected to drive the system insulating which we have checked with LDA+U calculation. The energy bands dominated by other d characters like d_{xy} , d_{yz} , d_{zx} and $d_{3z^2-r^2}$ are located in the energy range from -2.2 eV to -1.2 eV and the O-p dominated bands appear in the energy range from -4 eV to -1.2 eV. The contribution of O₂ character in the conduction bands crossing the Fermi level is small (see inset of Fig-4) compared to other oxygens because of the large Cu-O₂ bond length. Te1 and Te2-p states which remain primarily empty have non-negligible contribution to the bands crossing the Fermi energy and play useful role in mediating the Cu-Cu exchange interaction as will be discovered in the following.

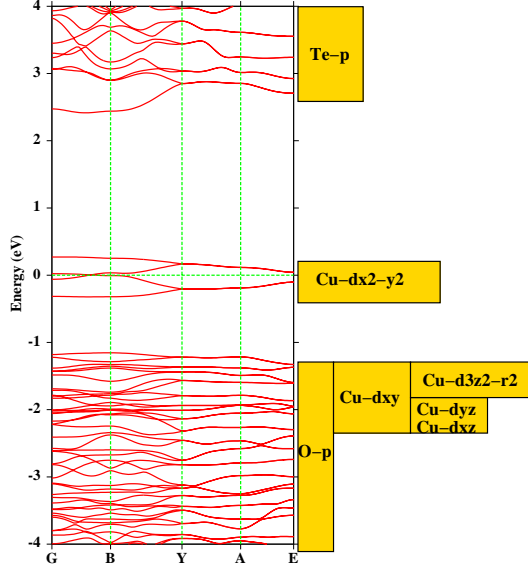


FIG. 3: LDA band dispersion of CuTe_2O_5 plotted along various symmetry directions. The dominant orbital contributions in various energy ranges are shown in boxes on the right-hand side. The various Cu-d characters are shown in local coordinate system with the local z-axis pointing along Cu-O₂ bond and local y-axis pointing approximately along the Cu-O₅ bond.

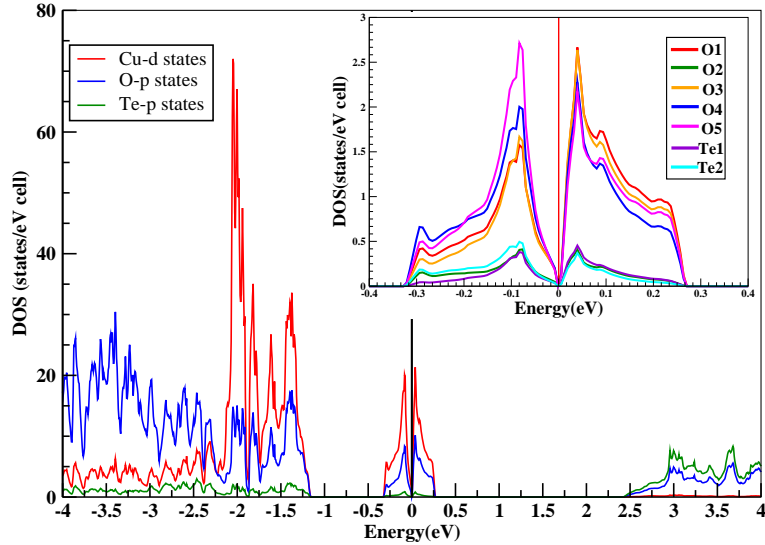


FIG. 4: Partial density of states of Cu-*d*, O-*p* and Te-*p* orbitals, for CuTe_2O_5 . Inset show the density of states for O1-*p*, O2-*p*, O3-*p*, O4-*p*, O5-*p*, Te1-*p*, Te2-*p* orbitals in the energy range close to E_f

IV. LOW ENERGY HAMILTONIAN

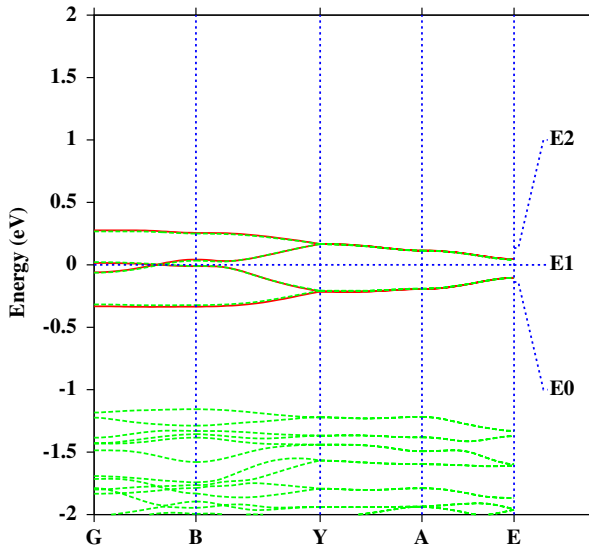
A powerful technique to construct a low-energy, tight binding (TB) Hamiltonian starting from a LDA band structure, is given by the NMTO downfolding method⁵. This method derives the low-energy Hamiltonian by energy selective, downfolding process that integrates out the high energy degrees of freedom. The low energy Hamiltonian is then defined in the basis of effective orbitals constructed via integration out process. This process takes into account the proper renormalization effect from the orbitals that are being downfolded. The accuracy of such process can be tuned by the choice of the number of energy points (N), used for selection of downfolded bands. If the low-energy bands form an isolated set of bands, the constructed effective orbitals, the NMTOs, span the Hilbert space of Wannier functions or in other words, the effective orbitals are the Wannier functions corresponds to the low-energy bands. The

TABLE I: Cu-Cu hopping parameters corresponding to the downfolded Cu- $d_{x^2-y^2}$ Hamiltonian

hopping	Cu-Cu distances in Å	Hopping parameters in meV
t_1	3.18	38.7
t_3	5.32	11.0
t_4	5.58	112.9
t_5	5.83	13.7
t_6	6.20	59.9
t_7	6.43	4.9

real space representation of the downfolded Hamiltonian $H = \sum t_{ij}(c_i^\dagger c_j + h.c)$ in the Wannier function basis gives the various hopping integrals t_{ij} between the effective orbitals.

For the present compound we have derived the low energy Hamiltonian defined in the basis of the effective Cu- $d_{x^2-y^2}$ orbitals, by keeping only the $d_{x^2-y^2}$ orbital for each Cu atom in the unit cell and integrating out all the rest. We show the downfolded bands in Fig-5 in comparison to the full LDA band structure. With the choice of three energy points E_0 , E_1 and E_2 . The downfolded bands are indistinguishable from the Cu- $d_{x^2-y^2}$ dominated bands of the full LDA calculation.

FIG. 5: Bands obtained with downfolded Cu- $d_{x^2-y^2}$ basis (solid lines) compared to full LDA band structure (dashed lines).

The corresponding Wannier function is plotted in Fig-6. The central part has the $3d_{x^2-y^2}$ symmetry with the choice of the local coordinate system as stated above, while the tails are shaped according to O- p_x/p_y . Cu- $d_{x^2-y^2}$ orbital form strong pd σ antibonds with the O- p_x/p_y tails. O- p_x/p_y tails bend towards the Te2 atom, which indicates the importance of hybridization effect from the Te cations and enhances the Cu-Cu interaction placed at different structural dimer Cu₂O₁₀.

Table-I shows the various dominant effective hopping integrals t_{ij} (having magnitude ≥ 1 meV) between the Cu²⁺ ions at sites i and j. The notation for the hopping are shown in Fig-7. In Fig-7a we show dominant interactions in the bc plane. The strongest interaction, t_4 , is found to be between those two Cu²⁺ ions which are situated at different structural dimer (Cu₂O₁₀) and the interaction is mediated by two O-Te-O bridges. t_1 , which represent the interaction between two Cu²⁺ ions situated within the same structural dimer unit, is 1/3 of the strongest interaction (t_4). The second strongest interaction, t_6 , mediated by one O-Te-O bridge is about 1/2 of the interaction t_4 . Fig-7b shows the interaction paths in ab plane, which are weak in general and may be neglected. Specifically as example we mention the interactions t_3 and t_7 , which are approximately 1/10 and 1/25 of the strongest interaction (t_4) respectively. In the following we discuss the origin of various dominant interaction paths.

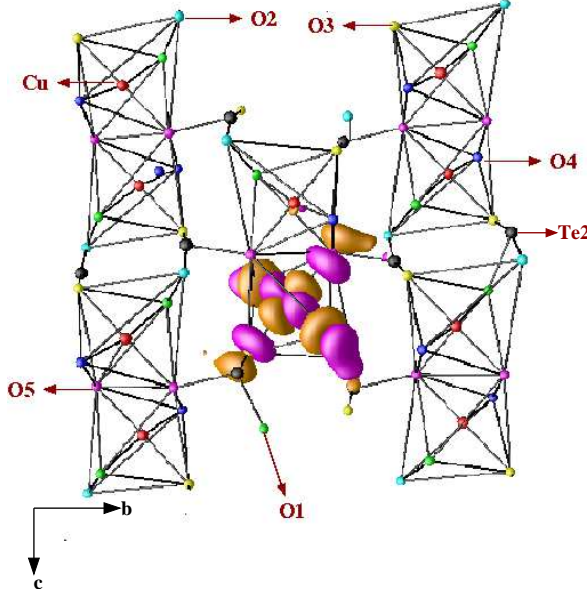


FIG. 6: Effective $Cu d_{x^2-y^2}$ orbital with lobes of opposite signs colored as orange and magenta. The $d_{x^2-y^2}$ orbital is defined with the choice of local coordinate system with local z-axis pointing along Cu-O2 bond and local y-axis pointing approximately along the Cu-O5 bond.

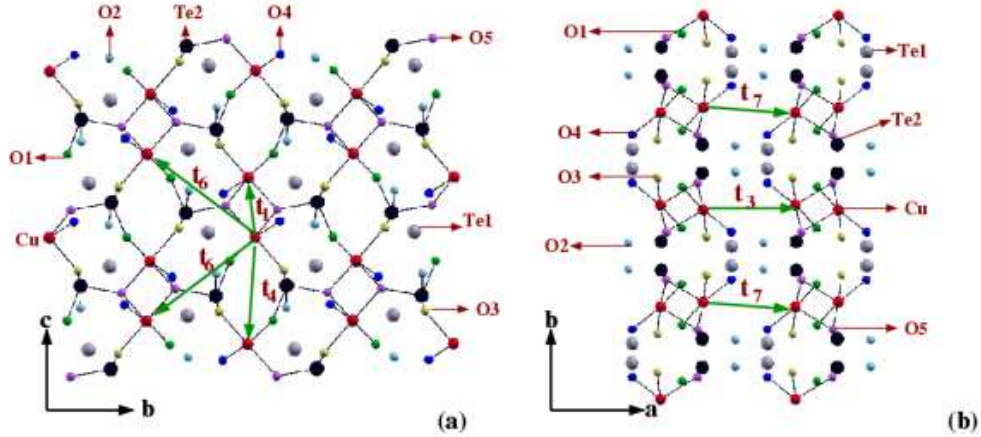


FIG. 7: Different interaction paths of effective Cu-Cu interactions

A. Strongest interaction (Structural interdimer interaction)- t_4

The strongest interaction, t_4 , mediated by two O-Te-O bridges produce Cu-O-Te-O-Cu supersuperexchange (SSE) interaction generating the spin-spin coupling J_4 . The strength of a SSE interaction through the exchange path of type Cu-O-L-O-Cu (e.g., L=Te) depends sensitively on how the O-L-O linkage orients the two magnetic orbitals (i.e. the $d_{x^2-y^2}$ orbitals) centered at two Cu sites and also on how the tails of the magnetic orbitals, contributed by the orbitals of the ligand atom L, are oriented with respect to the central part⁶. In Fig-8 we show the Wannier function plot, where the effective Cu- $d_{x^2-y^2}$ like Wannier orbitals are placed at the Cu sites between which we have found the strongest interaction. The O- p_x/p_y tails bend towards the Te atoms in both the O-Te-O ligands and becomes responsible for the strong Cu-Cu bonding between two Cu^{2+} ions belonging to the different structural dimers.

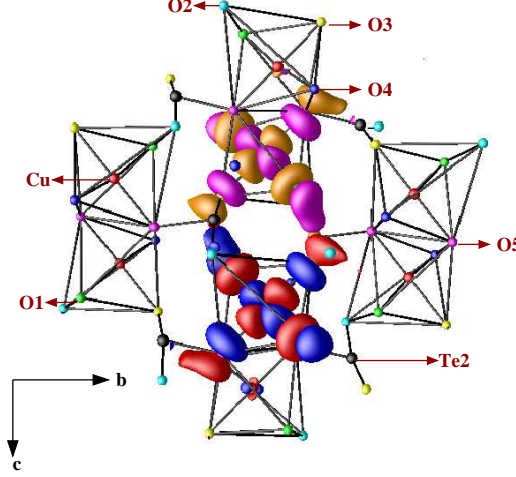


FIG. 8: Effective orbital corresponding to the downfolded NMTOs, placed at two Cu sites situated at two different structural dimer units corresponding to t_4 interaction.

B. Second strongest interaction (Structural interdimer interaction)- t_6

The hopping integral t_6 corresponds to the next strong Cu-Cu interaction, which is mediated via one O-Te-O bridge and responsible for the Cu-O-Te-O-Cu SSE generating the spin-spin coupling J_6 . Fig-9 shows the Wannier plots of the Cu- $d_{x^2-y^2}$ downfolded NMTOs, situated at two Cu sites between which we have found as the second strongest interaction. Again the oxygen tails bend towards the interconnecting TeO₂ unit to provide a interaction pathway between the two Cu²⁺ sites.

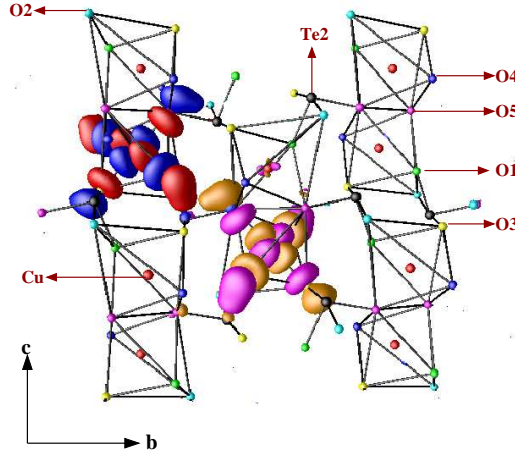


FIG. 9: Effective orbital corresponding to the downfolded NMTOs, placed at two Cu sites situated at two different structural dimer units corresponding to t_6 interaction.

C. Structural intradimer interaction- t_1

t_1 corresponds to intradimer Cu-Cu interaction which is mediated by O5-O5' atoms. In Fig-10 we show the Wannier function plot, where the effective Cu- $d_{x^2-y^2}$ like Wannier orbitals are situated at the Cu sites of same structural dimer unit. As we stated above, each structural dimer units are made of two edge sharing CuO₆ distorted octahedra. In the case of first octahedron O5 is situated on the basal plane of the octahedron and O5-p_x/p_y form pd σ antibond with the Cu- $d_{x^2-y^2}$ orbital, where as O5' is situated at the apical position for this octahedron. Reverse is true for the second octahedron. Therefore Cu- $d_{x^2-y^2}$ orbitals of two Cu²⁺ sites placed at the same structural dimer unit are misaligned, which is responsible for the weak Cu-Cu intradimer interaction. As the Cu-O5-Cu and Cu-O5'-Cu angles turn out to be 96.76 degree in both cases, the Cu-Cu interaction within the structural dimer, which is weak, may be of ferromagnetic type.

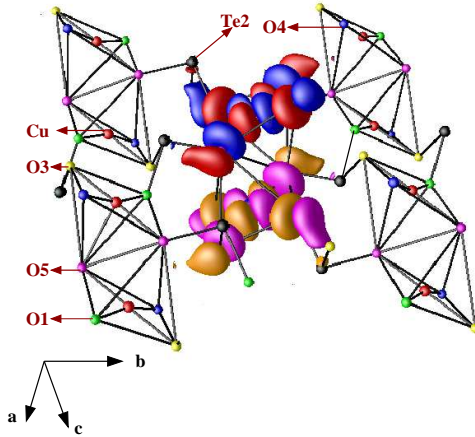


FIG. 10: Cu- $d_{x^2-y^2}$ downfolded NMTOs, placed at two Cu sites situated within same structural dimer. The O2 sites with long Cu-O2 bond lengths have been removed from the plot for better view.

V. CONCLUSION

Our first-principles NMTO-downfolding study reveals that the strongest Cu-Cu interaction is given by the Cu pairs belonging to different structural dimer units, and connected by two O-Te-O bridges (t_4). This interaction is found to be most dominant, along with two additional in-plane Cu-Cu interactions, one of which is that of the Cu pairs belonging to the same structural dimer unit (t_1). This is contrary to recent study by Deisenhofer *et al*, which represented the CuTe₂O₅ system as alternating spin chain system with strong intra and inter dimer coupling, the exchange dimer with strongest interaction being that connected via the interaction path given by t_6 . Based on our results we propose a 2D coupled dimer model for CuTe₂O₅. The Quantum Monte Carlo (QMC) study based on our predicted model to compute the spin susceptibility which can be compared with experiment, is on the way.

VI. ACKNOWLEDGMENT

We would like to thank P. Lemmens and J. Deisenhofer for discussions and for bringing the problem into our attention. We acknowledge Roser Valenti for her active participation in the discussions and future ongoing collaboration.

VII. REFERENCES

- ¹ P. Lemmens, G. Guntherodt, C. Gros, Phys. Rep. **375**, 1(2003)
- ² J. Deisenhofer et.al. Phys. Rev. B **74**, 174421(2006)
- ³ K. Hanke, V. Kupcik, O. Lindqvist, Acta Cryst. B **29**, 963(1973)
- ⁴ O. K. Andersen, Phys. Rev. B, **12**(1975) 3060
- ⁵ O. K. Andersen and T. Saha-Dasgupta, Phys. Rev. B **62**, R16219(2000)
- ⁶ M. -H. Whangbo, H. -J. Koo, and D. J. Dai, Solid State Chem. **176**, 417 (2003); M. -H. Whangbo, D. J. Dai and H. -J. Koo, Solid State Sci. **7**, 827(2005)